# NMR probe of pseudogap characteristics in $CaAl_{2-x}Si_{2+x}$

C. S. Lue,* S. Y. Wang, and C. P. Fang
*Department of Physics, National Cheng Kung University, Tainan 701, Taiwan*
(Received 13 February 2007; published 15 June 2007)

We report the results of a $^{27}$Al nuclear magnetic resonance (NMR) study of $CaAl_{2-x}Si_{2+x}$, near the stoichiometric composition with $x=0$. The low-temperature NMR relaxation rates for stoichiometric ($x=0$) and nonstoichiometric ($x=-0.1$ and 0.1) compounds follow a Korringa law, associated with a finite density of carriers at the Fermi level. High-temperature relaxation rates for $x \geqslant 0$ go over to a semiconductorlike activated form, providing information about the electronic structure near the Fermi energy. The results are consistent with pseudogap features identified by recent band-structure calculations. An analysis of the pseudogap change vs composition further points out that the band-filling picture is proper for the understanding of the NMR observations in $CaAl_{2-x}Si_{2+x}$.

DOI: 10.1103/PhysRevB.75.235111 PACS number(s): 76.60.−k, 71.55.Ak, 71.20.−b

## I. INTRODUCTION

After the discovery of superconductivity in $MgB_2$, there has been of great interest in related compounds with hexagonal graphitelike $AlB_2$-type structure.[1–3] The layered ternary alumino silicides Ca-Al-Si have, thus, attracted considerable attention because one of the systems CaAlSi, isostructural to $MgB_2$, is also a superconductor with $T_C$ of about 7.8 K.[3,4] In addition to CaAlSi, there is another ternary layered Ca-Al-Si system, $CaAl_2Si_2$, which crystallizes in the trigonal $La_2O_3$-type structure (space group: $P\bar{3}m1$). Within this crystal structure, Si and Al atoms are arranged in the chemically ordered double-corrugated hexagonal layers, with Ca atoms alternating between them (see Fig. 1). Unlike CaAlSi, no evidence of superconducting behavior has been observed above 1.4 K in $CaAl_2Si_2$. The electrical difference between these two Ca-Al-Si systems has been associated with the significant variation in their electronic structures:[5–7] CaAlSi is an ordinary metal in the normal state, while $CaAl_2Si_2$ is a semimetal with a pseudogap at the Fermi level ($E_F$). In fact, a recent Hall coefficient measurement on $CaAl_2Si_2$ showed a sign reversal at around 150 K, indicative of a change of dominant carrier with temperature.[8] According to the electronic structure calculation on $CaAl_2Si_2$,[7] the peculiar transport behavior has been attributed to the semimetallic response, as the low-$T$ behavior is dominated by the intrinsically metallic nature, while the high-$T$ feature is attributed to a thermally activated increase in the density of carriers of different types.

A pseudogap appearing at the Fermi level is a common occurrence in transition metal-metalloid compounds.[9] There have been considerable advances in understanding how a gap may form in the region of the Fermi level, due to hybridization between $d$ and $s$-$p$ states.[10,11] Quasicrystalline materials, typically composed of transition metal-metalloid constituents, also feature Fermi-level pseudogaps which dominate the electronic properties of the materials.[12] In this paper, we examine the electronic states in the pseudogap region of $CaAl_{2-x}Si_{2+x}$ by means of the nuclear magnetic resonance (NMR) spectroscopy. We have investigated alloys with $x=-0.1$, 0, and 0.1, in order to understand how the semimetallic nature behaves under doping with excess Al or Si.

## II. EXPERIMENTAL DETAILS

Samples studied here were prepared from 99.9% Ca, 99.9% Al, and 99.9999% Si by mixing appropriate amounts of elemental metals. They were placed in a water-cooled copper crucible and then were melted several times in an Ar arc-melting furnace. The resulting ingots were annealed in a vacuum-sealed quartz tube at 800 °C for two days, followed by furnace cooling. A Cu $K\alpha$ x-ray analysis on powdered samples is consistent with the expected $La_2O_3$-type structure. Several weak peaks remain unidentified which had little effect on the NMR measurements.

NMR experiments were performed using a Varian 300 spectrometer, with a constant field of 7.05 T. A home-built probe was employed for both room-temperature and low-temperature measurements. Since the studied materials are metals or semimetals, powder samples were used to avoid the skin depth problem of the rf transmission power. Each specimen was put in a plastic vial that showed no observable $^{27}$Al NMR signal.

### A. Powder patterns

Central transition $\left(m=\frac{1}{2}\leftrightarrow-\frac{1}{2}\right)$ line shapes were obtained from spin-echo fast Fourier transforms using a standard $\pi/2-\tau-\pi$ sequence. The ordered $La_2O_3$-type structure contains a single Al site which is axially symmetric, leading to a one-site NMR spectrum. The observed $^{27}$Al room-temperature powder patterns for all $CaAl_{2-x}Si_{2+x}$ alloys are shown in Fig. 2. The line shapes here are manifested by the

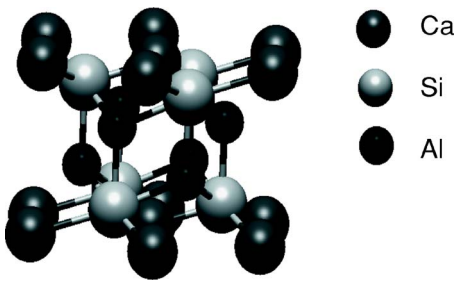


FIG. 1. (Color online) Crystal structure of $CaAl_2Si_2$.

 

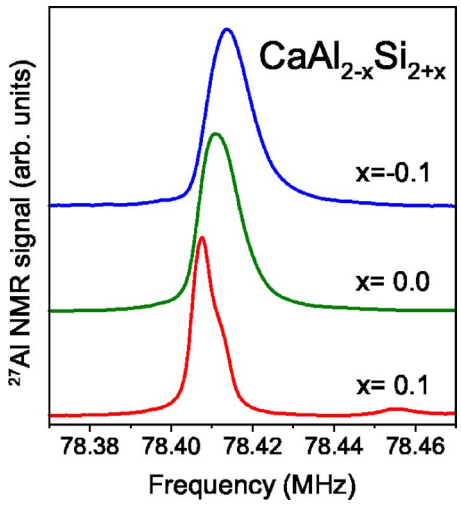


FIG. 2. (Color online) $^{27}$Al central transition spectra for $CaAl_{2-x}Si_{2+x}$ measured at room temperature.

simultaneous presence of anisotropic Knight shift and second-order quadrupole effects. Due to electric quadrupole coupling, the $^{27}$Al NMR spectrum $\left(I=\frac{5}{2}\right)$ consists of four satellite lines, as illustrated in Fig. 3. For the powder specimens, as in our experiment, these lines exhibit as a typical powder pattern, with distinctive edge structures corresponding to the quadrupole parameter. Since the first-order quadrupole shift is the main effect shaping the satellite lines, the quadrupole frequency $\nu_Q$ was determined directly from these lines. For the present $CaAl_{2-x}Si_{2+x}$, $\nu_Q=0.36\pm0.02$ MHz remains unchanged with the composition $x$, indicating that the local electric environments are almost the same for these materials.

### B. Knight shifts

In Fig. 4, we display the temperature dependence of the observed $^{27}$Al Knight shifts ($K$'$s$) for $CaAl_{2-x}Si_{2+x}$, indicated by open squares, solid circles, and open triangles for $x=-0.1$, 0, and 0.1, respectively. Here, the value of $K$ was determined from the position of the maximum of each spectrum with respect to an aqueous $AlCl_3$ solution reference. For $CaAl_{2.1}Si_{1.9}$, $K$ shows nearly $T$-independent behavior at

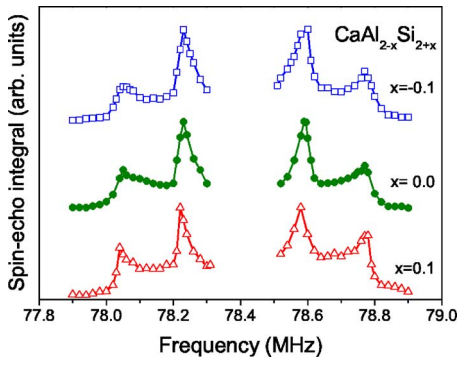


FIG. 3. (Color online) Fully resolved $^{27}$Al NMR satellite line shapes for $CaAl_{2-x}Si_{2+x}$.

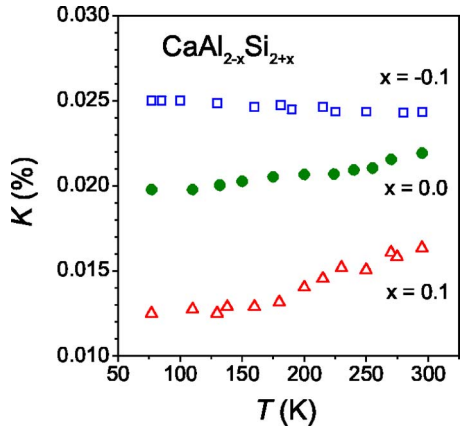


FIG. 4. (Color online) Temperature dependence of the observed $^{27}$Al Knight shifts for $CaAl_{2-x}Si_{2+x}$.

all temperatures, a typical characteristic for nonmagnetic metals. On the other hand, the Knight shifts of $CaAl_2Si_2$ and $CaAl_{1.9}Si_{2.1}$ clearly exhibit a shift to higher frequencies with increasing temperature in addition to a low-$T$ constant term. Such a phenomenon is commonly seen in ordinary semimetals as the low-$T$ behavior is dominated by the intrinsically metallic nature, while the high-$T$ feature arises from an exotic response.

For each individual compound, the $T$-independent term can be associated with the Fermi-contact Knight shift ($K_s$) which is connected to the number of the $s$-character carriers in the ground state.[13] The tiny $K_s$ values (see Table I) for all studied materials suggest little Al-$s$ density of states (DOS) in the vicinity of the Fermi level, being consistent with the results from band-structure calculations.[7] The $T$-dependent Knight shift reflects an increase in the spin susceptibility, attributed to a thermally activated increase in the density of carriers, also responsible for the enhancement in the relaxation rate.

### C. Spin-lattice relaxation rates

Temperature dependence of the spin-lattice relaxation rate $(1/T_1)$ was measured using the inversion recovery method. We recorded the signal strength by integrating the recovered spin-echo signal. In this experiment, the relaxation process involves the adjacent pairs of spin levels, and the corresponding spin-lattice relaxation is a multiexponential expression.[14] $T_1$ values were thus obtained by fitting to a multiexponential recovery curve for $I=5/2$. In Fig. 5, we

TABLE I. Fermi-contact Knight shift, Korringa constant, Fermi-level $s$-DOS in units states/eV cell, and energy splitting of $CaAl_{2-x}Si_{2+x}$.

| $x$ | $K_s$ (%) | $1/(T_{1K}T)$ ($s^{-1}$ $K^{-1}$) | $N_s$ ($E_F$) | $\Delta$ (meV) |
|---|---|---|---|---|
| −0.1 | 0.025 | $21.7\times10^{-4}$ | $5.8\times10^{-3}$ | |
| 0 | 0.020 | $7.6\times10^{-4}$ | $3.4\times10^{-3}$ | 58 |
| 0.1 | 0.013 | $5.6\times10^{-4}$ | $3.0\times10^{-3}$ | 172 |

show a plot of $1/T_1$ versus temperature for the studied $CaAl_{2-x}Si_{2+x}$ alloys. For all compositions, the low-$T$ $1/T_1$'s exhibit a constant $T_1T$ behavior, confirming a Korringa relaxation process at low temperatures. From a straight-line fit, we obtained $1/T_{1K}T=2.2\times10^{-3}$, $7.6\times10^{-4}$, and $5.6\times10^{-4}$ $s^{-1}$ $K^{-1}$ for $x=-0.1$, 0, and 0.1, respectively, where the subscript $K$ denotes the Korringa process. Normally, the spin contribution to $1/T_{1K}T$ can be used to evaluate the Fermi-level DOS, and we will discuss these results in the next section.

Above 150 K, $1/T_1$ rises rapidly for $CaAl_2Si_2$ and $CaAl_{1.9}Si_{2.1}$, with an activated temperature dependence. This is the characteristic behavior for semiconductors,[15] with the increase in relaxation rate due to an increase in the number of carriers because of thermal excitation across an energy gap. Thus, it is easy to reconcile the metallic behavior observed at low temperatures with the high-$T$ semiconducting behavior by assuming a two-band model, with one band overlapping the Fermi level while the second band is separated from the Fermi level by an energy gap, $\Delta$. In this case, the relaxation rate is given by[15]

$$\frac{1}{T_1T}=\frac{1}{T_{1K}T}+CTe^{-\Delta/k_BT}, \tag{1}$$

where $1/T_{1K}T$ is the Korringa value obtained above, and the second term is due to the band edge separated from the Fermi level. This form assumes an effective-mass approximation for the band edge, with $C$ associated with the effective mass of carriers as well as their concentrations. Each carrier density varies with temperature according to $T^{3/2}\exp(-\Delta/2k_BT)$. The $T_{1K}T$ value was obtained from the low-temperature fit as mentioned above, and we found that Eq. (1) gives good agreement with the data of $CaAl_2Si_2$ and $CaAl_{1.9}Si_{2.1}$, shown as the dashed curves in Fig. 5. The values of energy gap extracted from these fits are recorded in Table I. Note that $1/T_1$ for $CaAl_{1.9}Si_{2.1}$ follows a Korringa relation at all temperatures, indicating that the Fermi level has moved out of the pseudogap for that material.

## III. DISCUSSION

The Korringa contributions to $1/T_1$ can be evaluated to provide a measure of Al-$s$ Fermi-level DOS as reported previously for other aluminides.[16–18] For the present alloys, the relaxation of Al nuclei is dominated by their coupling to the spin of the $s$-character electrons. In the absence of the collective electron effects, the relaxation rate is simply governed by the initial occupied and final unoccupied electronic states, associated with the hyperfine field arising from contact electrons. Under such approximation, the spin-lattice relaxation rate can be written as[19]

$$\frac{1}{T_{1K}T}=2hk_B[\gamma_nH_{hf}^sN_s(E_F)]^2q, \tag{2}$$

where $h$, $k_B$, and $T$ are the Planck constant, Boltzmann constant, and absolute temperature, respectively. $\gamma_n$ is the Al nuclear gyromagnetic ratio, $H_{hf}^s$ is the hyperfine field per electron of the Al-$s$ electrons at the Fermi level, and $N_s(E_F)$ represents the $s$-DOS at the Fermi level. Here, $q$ is a factor equal to the reciprocal of the degeneracy. As indicated in Table I, the deduced $(1/T_{1K}T)$'s were found to be much smaller than that of CaAlSi, which is about 0.063 $s^{-1}$ $K^{-1}$.[20] The strong reduction of $1/T_{1K}T$ is related to the small Fermi-level DOS for $CaAl_{2-x}Si_{2+x}$, consistent with the prediction given from theoretical calculations.[7]

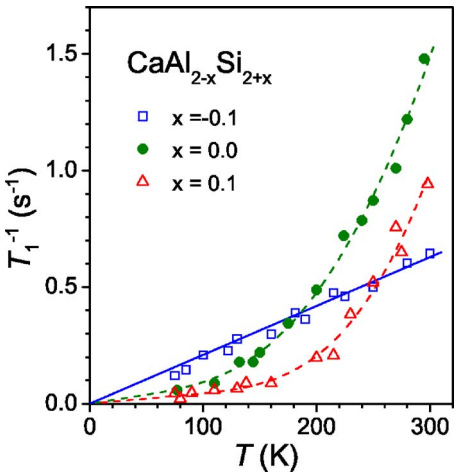


FIG. 5. (Color online) Temperature variation of the $^{27}Al$ spin-lattice relaxation rates for $CaAl_{2-x}Si_{2+x}$. The solid line represents a fit to the Korringa behavior for $CaAl_{2.1}Si_{1.9}$. Dotted curves: fit to the semimetallic character from Eq. (1) for $CaAl_2Si_2$ and $CaAl_{1.9}Si_{2.1}$.

For the stoichiometric $CaAl_2Si_2$, band-structure calculations[7] indicated little but nonzero Al Fermi-level DOS near the top of the hole pockets which would dominate the $^{27}Al$ relaxation. Furthermore, these pockets have degeneracy of 2, giving $q=1/2$. Since $p$ and $d$ hyperfine fields are generally an order of magnitude smaller than the $s$-character hyperfine field,[21] the main hyperfine field in the studied alloys arises from contact electrons. Taking $H_{hf}^s\sim1.9\times10^6$ G calculated for Al metal,[22] we obtain $N_s(E_F)=0.0034$ states/eV cell for $CaAl_2Si_2$, which can be compared to $N_s(E_F)=0.022$ states/eV cell measured in the same way in CaAlSi.[20] It is apparent that the number of carriers in $CaAl_2Si_2$ is much less than in CaAlSi, which is consistent with the transport measurements showing the Hall coefficient of $CaAl_2Si_2$ greater than that of CaAlSi by one order of magnitude.[8]

In the reciprocal space near the $\Gamma$ point, another valence-band edge just below $E_F$ appears in $CaAl_2Si_2$ (measured from Fig. 1 in Ref. 7). We consider that the separation of this band edge from $E_F$ is responsible for the thermal excitations in both the Knight shift and $T_1$ of $CaAl_2Si_2$. As a matter of fact, the tiny energy splitting $\Delta=58$ meV, deduced from the activated behavior of $T_1$, seems to be in satisfactory agreement with the band calculation.

In a simple rigid-band model, each additional Si should contribute more electrons in the mixed alloys. As a result, $E_F$ shifts up with respect to the position of $CaAl_2Si_2$, leading to a reduction of $N_s(E_F)$ but an increase of the energy gap, as indeed observed for $CaAl_{1.9}Si_{2.1}$. On the opposite side, substituting Al onto Si sites would add more holes in the valence bands, moving $E_F$ well outside the pseudogap region. It,

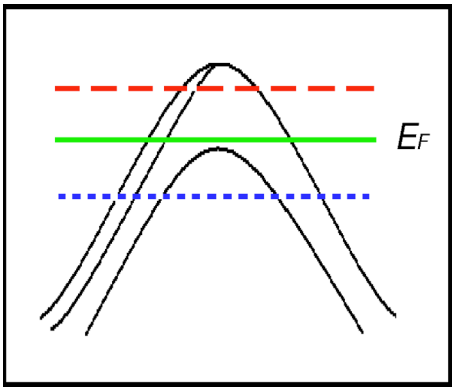


FIG. 6. (Color online) Schematic illustration of the hole pockets near the Γ point, reproduced from the band calculations for $CaAl_2Si_2$ (Ref. 7). The Fermi level is denoted as $E_F$ (solid line) for the stoichiometric $CaAl_2Si_2$, and the dotted and dashed lines correspond to the shifted $E_F$'s for $CaAl_{2.1}Si_{1.9}$ and $CaAl_{1.9}Si_{2.1}$, respectively.

thus, yields a larger $N_s(E_F)$ and a disappearance of the gap feature, resulting in the absence of an activated response for $CaAl_{2.1}Si_{1.9}$. Such a picture is schematically illustrated in Fig. 6.

It is worthwhile mentioning that a recent Seebeck coefficient ($S$) measurement on $CaAl_{2-x}Si_{2+x}$ also exhibits a similar tendency.[23] As compared to the magnitude of $S$ in $CaAl_2Si_2$, an enlargement of the electron pocket along with a reduction of the hole ones due to an upward shift of $E_F$ is responsible for the increase of $S$ value in $CaAl_{1.9}Si_{2.1}$. On the other hand, the decrease of $S$ value in $CaAl_{2.1}Si_{1.9}$ could be associated with a downward shift of $E_F$ as a partial replacement of Si by Al in $CaAl_2Si_2$.

Therefore, the NMR observations are in reasonably agreement with the results of band theory for these alloys. We find all compositions studied to be metallic or semimetallic, with pseudogap signature evident in the relaxation behavior for $CaAl_2Si_2$ and $CaAl_{1.9}Si_{2.1}$. It is worth comparing the present results with those found in the Heusler-type compounds $Fe_2VAl$ and $Fe_2VGa$, which also attracted considerable interest due to indications of pseudogap behavior.[24,25] Both materials are semimetals and band-structure calculations revealed pseudogap features arising from a slight overlap between conduction and valence bands.[9,26–28] Accordingly, the electronic characteristics of these systems are very similar to the case of $CaAl_{2-x}Si_{2+x}$, which allows us to classify these materials to the common group of intermetallics with a pseudogap at the Fermi surface.

## IV. CONCLUSIONS

NMR measurements have provided a local picture of the electronic properties of $CaAl_{2-x}Si_{2+x}$, indicating that $CaAl_2Si_2$ is essentially semimetallic, with properties quite similar to those calculated via band-structure methods. The Knight shifts and spin-lattice relaxation rates are understood in terms of semimetallic characteristics, with a small band overlap at the Fermi level falling within a pseudogap formed by nearby bands. Changes of the band-edge features of the pseudogap evidenced by the NMR relaxation measurements can be interpreted well by a simple rigid-band scenario.

## ACKNOWLEDGMENT

We are grateful for the support from the National Science Council of Taiwan under Grant No. NSC-95-2112-M-006-021-MY3 (C.S.L).

*Email address: cslue@mail.ncku.edu.tw.

[1] J. Nagamastu, N. Nakagawa, T. Muranaka, Y. Zenitani, and J. Akimtsu, Nature (London) **410**, 63 (2001).
[2] M. Imai, E. Abe, J. Ye, K. Nishida, T. Kimura, K. Honma, H. Abe, and H. Kitazawa, Phys. Rev. Lett. **87**, 077003 (2001).
[3] Motoharu Imai, Kenji Nishida, Takashi Kimura, and Hideki Abe, Appl. Phys. Lett. **80**, 1019 (2002).
[4] B. Lorenz, J. Lenzi, J. Cmaidalka, R. L. Meng, Y. Y. Sun, Y. Y. Xue, and C. W. Chu, Physica C **383**, 191 (2002).
[5] I. I. Mazin and D. A. Papaconstantopoulos, Phys. Rev. B **69**, 180512(R) (2004).
[6] G. Q. Huang, L. F. Chen, M. Liu, and D. Y. Xing, Phys. Rev. B **71**, 172506 (2005).
[7] G. Q. Huang, M. Liu, L. F. Chen, and D. Y. Xing, J. Phys.: Condens. Matter **17**, 7151 (2005).
[8] M. Imai, H. Abe, and K. Yamada, Inorg. Chem. **43**, 5186 (2004).
[9] M. Weinert and R. E. Watson, Phys. Rev. B **58**, 9732 (1998).
[10] J. F. van Acker, E. W. Lindeyer, and J. C. Fuggle, J. Phys.: Condens. Matter **3**, 9579 (1991).
[11] A. P. Malozemoff, A. R. Williams, and V. L. Moruzzi, Phys. Rev. B **29**, 1620 (1984).
[12] T. Klein, O. G. Symko, D. N. Davydov, and A. G. M. Jansen, Phys. Rev. Lett. **74**, 3656 (1995).
[13] C. P. Slichter, *Principles of Magnetic Resonance* (Springer-Verlag, New York, 1990).
[14] W. W. Simmons, W. J. O'Sullivan, and W. A. Robinson, Phys. Rev. **127**, 1168 (1962).
[15] N. Bloembergen, Physica (Amsterdam) **20**, 1130 (1954); Dieter Wolf, *Spin Temperature and Nuclear-Spin Relaxation in Matter* (Clarendon, Oxford, 1979).
[16] C.-S. Lue, S. Chepin, J. Chepin, and Joseph H. Ross, Jr., Phys. Rev. B **57**, 7010 (1998).
[17] C. S. Lue, B. X. Xie, S. N. Horng, J. H. Su, and J. Y. Lin, Phys. Rev. B **71**, 195104 (2005).
[18] C. S. Lue, J. Y. Lin, and B. X. Xie, Phys. Rev. B **73**, 035125 (2006).
[19] J. Korringa, Physica (Amsterdam) **16**, 601 (1950).
[20] C. S. Lue, B. X. Xie, and C. P. Fang, Phys. Rev. B **74**, 014505 (2006).
[21] *Metallic Shifts in NMR*, edited by G. C. Carter, L. H. Bennett, and D. J. Kahan (Pergamon, Oxford, 1977).

[22] G. C. Carter, I. D. Weisman, L. H. Bennett, and R. E. Watson, Phys. Rev. B **5**, 3621 (1972).
[23] Y. K. Kuo, K. M. Sivakumar, J. I. Tasi, C. S. Lue, J. W. Huang, S. Y. Wang, D. Varshney, N. Kaurav, and R. K. Singh, J. Phys.: Condens. Matter **19**, 176206 (2007).
[24] C.-S. Lue and Joseph H. Ross, Jr., Phys. Rev. B **58**, 9763 (1998).
[25] C. S. Lue and Joseph H. Ross, Jr., Phys. Rev. B **63**, 054420 (2001).
[26] G. Y. Guo, G. A. Botton, and Y. Nishino, J. Phys.: Condens. Matter **10**, L119 (1998).
[27] D. J. Singh and I. I. Mazin, Phys. Rev. B **57**, 14352 (1998).
[28] Ruben Weht and W. E. Pickett, Phys. Rev. B **58**, 6855 (1998).